Structure of Alumina and Zirconia Nanoparticles Synthesized by the Karlsruhe Microwave Plasma Process

S. Schlabach[1], V. Szabó[1], D. Vollath[1], A. Braun[2] and R. Clasen[2]

[1] Forschungszentrum Karlsruhe GmbH, Institut für Materialforschung III, P.O.Box 3640, D-76021 Karlsruhe, Germany

[2] Universität des Saarlandes, Lehrstuhl für Pulvertechnologie von Glas und Keramik, P.O.Box 151150, D-66041 Saarbrücken, Germany

Keywords: Microwave Plasma Process, nanoparticles, zirconia, alumina.

Abstract. Applying the Karlsruhe Microwave Plasma Process, alumina and zirconia particles with particle sizes in the range from 2 to 5 nm were synthesized. Additionally, the influence of small amounts of iron(III)-oxide, chromia, and magnesia on the crystallization and phase transitions in alumina powders was investigated. It is shown that these dopants may influence the crystallization behavior significantly. Especially, the addition of 1 mol% iron(III)-oxide reduced the temperature of the formation of α-alumina from 1200 °C to 300 °C.

Introduction

Due to their small particle size, light scattering in nanomaterials is very small. Therefore, new materials for optoceramics based on nanosized particles are very promising. For this study, nanosized zirconia, alumina-coated zirconia, alumina, and alumina with iron(III)-oxide, chromia and magnesia additives were synthesized using the Karlsruhe Microwave Plasma Process [1, 2]. Focus of this work are synthesis and characterization of nanoparticles with respect to size and phase composition. The powders were characterized using transmission electron microscopy (TEM), x-ray diffraction (XRD), differential scanning calorimetry (DSC), thermo-gravimetry (TG), and high temperature x-ray diffraction (HT-XRD).

Karlsruhe Microwave Plasma Process.

The Karlsruhe Microwave Plasma Process is capable to produce non-agglomerated uncoated and coated nanoparticles [1, 2] with a narrow particle size distribution [3]. In this process, volatile halides, carbonyls, or organometallic precursors are vaporized in an argon stream and introduced into an argon/20 vol% oxygen microwave plasma, where oxide nanoparticles are formed. In situ coating of each single particle is possible, because the particles leave the plasma zone, where the reaction occurs, with electric charges of equal sign. Therefore, the particles repel each other. This avoids agglomeration and makes it possible to coat the particles in a further step. The addition of dopants to alumina was realized by mixing the appropriate precursors. The reactions were performed in quartz tubes passing the microwave cavities. In the system, the pressure was set to 10 mbar and the temperatures were between 250 and 500 °C. The reaction time in the plasma zone is in the range of 4 ms. These syntheses were performed using a frequency of 2.45 GHz (6 kW). Fig. 1 shows schematically the experimental setup.
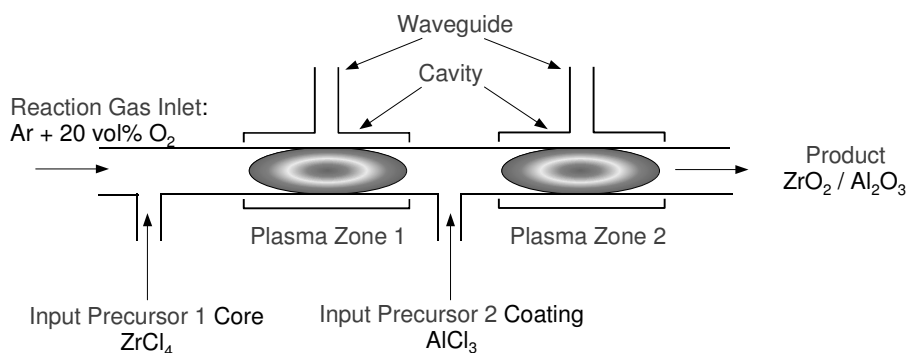
Fig. 1. Schematic experimental setup of the microwave plasma process for the synthesis of nanocomposites.

ZrO$_2$-powders.   Uncoated and alumina coated zirconia nanoparticles were synthesized using the Karlsruhe Microwave Plasma Process. TEM and XRD investigations show crystalline zirconia particles. In electron micrographs (111)-lattice fringes representing a well-crystallized material can be seen (Fig. 2). With XRD typical diffraction patterns for the cubic or tetragonal phase are obtained (Fig. 3). The alumina coating is amorphous. In electron micrographs (Fig. 2b), the coating is visible as faint halo around the zirconia particle. In the XRD spectrum (Fig. 3), there is no indication for crystalline alumina.

The particle sizes for both types of powders, uncoated and coated ones, are in the range from 2 to 5 nm (Fig. 2). Comparable values are obtained applying the Scherrer-formula to XRD and electron diffraction line profiles, respectively. In very rare cases, particles up to 10 nm may be found. In this case, the monoclinic zirconia phase occurs.
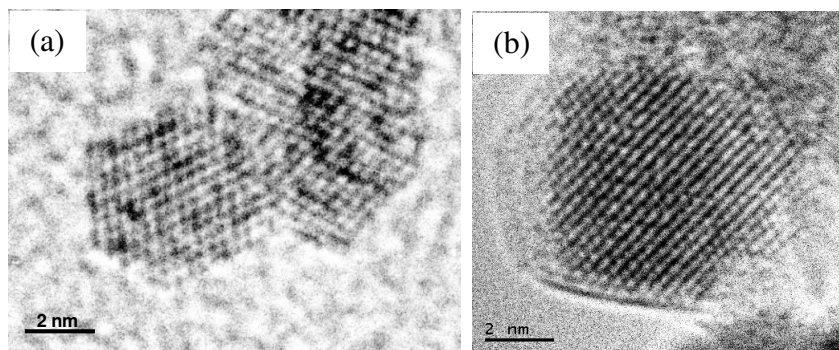

Fig. 2. TEM-images of bare (a) and alumina coated (b) zirconia nano-particles.

In both cases, zirconia is crystalline showing (111)-lattice fringes. The amorphous alumina coating is visible as a faint halo in Fig. 2b.
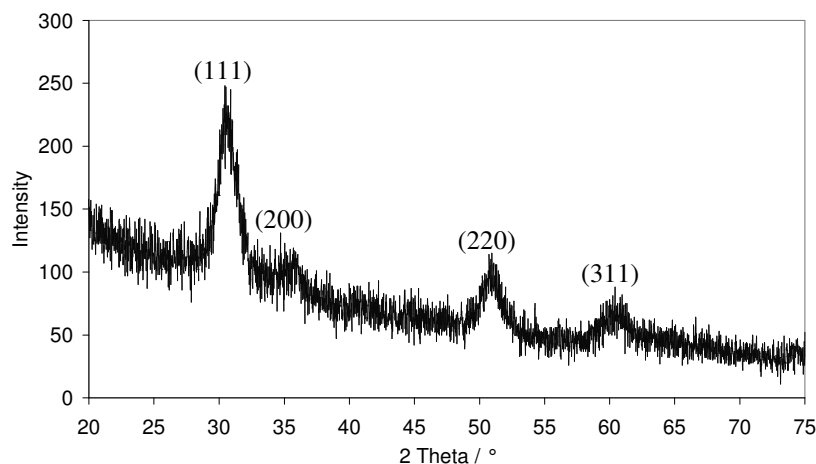

Fig. 3. XRD-spectrum of alumina coated zirconia.

The diffraction pattern indicates the tetragonal or cubic structure for the zirconia kernel, indications for crystallized alumina in the coating are not found.

Due to the line broadening, caused by the small particle sizes, in the XRD spectra and electron diffraction patterns it is not possible to distinguish between the cubic and the tetragonal phase of zirconia (Fig. 3). Additional investigations with EXAFS (extended x-ray-absorption fine structure analysis) clearly indicate the cubic structure (Table 1, [4]). The values obtained for nanosized zirconia are close to those of yttria-stabilized cubic zirconia and the ones calculated for the cubic phase. The splitting into two distinct Zr-O shells, evident in the tetragonal structure, is not observed.

EXAFS measurements show astonishingly low coordination numbers caused by high concentrations of Schottky defects (Table 1) corresponding perfectly with density values obtained by He-pycnometry (Table 2). The relative density of the zirconia nanoparticles is only 0.61.

	Nano-ZrO_2/Al_2O_3		Coarse $ZrO_2(Y_2O_3)$		Calculated cubic ZrO_2		Calculated tetragonal ZrO_2	
Shell	Zr-O	Zr-Zr	Zr-O	Zr-Zr	Zr-O	Zr-Zr	Zr-O	Zr-Zr
Radial distance $\pm \sigma$ [nm]	0.214 ±0.0076	0.365 ±0.0089	0.219 ±0.0087	0.360 ±0.010	0.2238	0.365	0.207 / 0.245	0.364 / 0.368
Coordination number	4.1	6.4	5.4	10.5	8	12	4 / 4	4 / 8

Table 1. Radial shell distances and coordination numbers for alumina coated nanosized zirconia particles compared with the data of coarse-grained cubic zirconia and calculated values of the cubic and tetragonal structure [4].

	Density [gcm^{-3}]		
	Nano-particles (He-pycnometry)	X-ray density	Rel. density
c-ZrO_2	3.8	6.21	0.61

Table 2. Density of zirconia particles

Al_2O_3-powders. Similar to zirconia powders, alumina powders show particle sizes in the range from 2 to 5 nm, in rare cases up to 10 nm (Fig. 4). Generally, alumina nanoparticles are amorphous; sometimes, small amounts of the cubic γ-phase are observed (Fig. 5a), correlated to the larger particles.
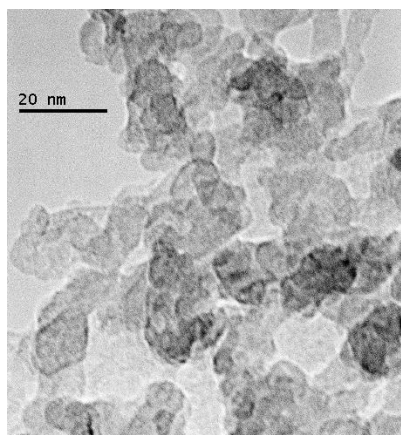

Fig. 4. TEM-image of alumina nanoparticles.

Additions of ~ 6 mol% iron(III)-oxide lead to a preference of the cubic γ-phase (Fig. 5b) in the as produced powder, whereas additions of chromia or magnesia show no effect on the crystallization behavior. Additionally, doping with iron(III)-oxide leads to a slightly yellow coloration of the powder.

Phase transitions to α-alumina determined with DSC and HT-XRD on amorphous alumina typically occur at temperatures of ~1200 °C (Fig. 6a) and ~1100 °C (Fig. 6b), respectively. The weight loss (Fig. 6a), observed with TG, is due to loss of surface water. Additions of ~1 mol% iron(III)-oxide causes a significant change in crystallization behavior. The temperature of the DSC signal attributed to the formation of α-alumina (Fig 7a) is reduced to 300 °C [5,6]. At higher temperatures, there is no further

indication for phase transitions. This surprisingly low temperature is proved with HT-XRD measurements (Fig. 7b) too. The α-phase is formed directly from the amorphous powder without transition through any metastable phase. Compacts made of this material, pressed uniaxially with 500 MPa, are sintered to a nearly transparent alumina ceramic at 900 °C [7].
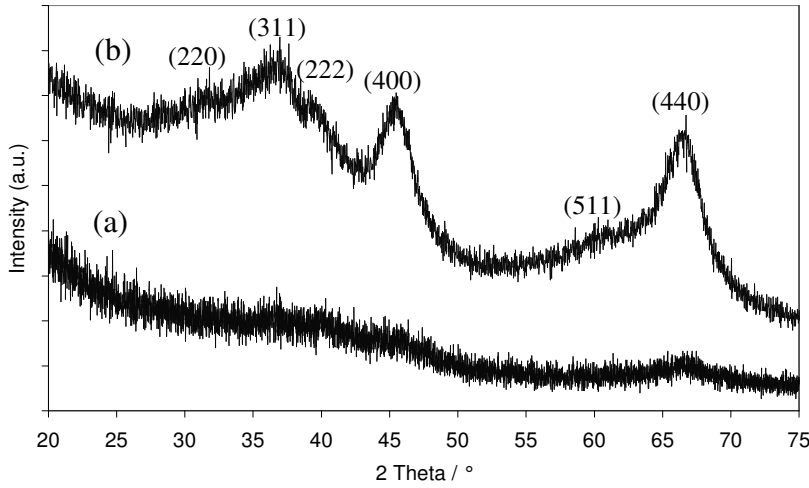

Fig. 5. XRD-spectra of as produced nanosized alumina particles.
(a) For pure alumina, only small amounts of the cubic γ-phase are found.
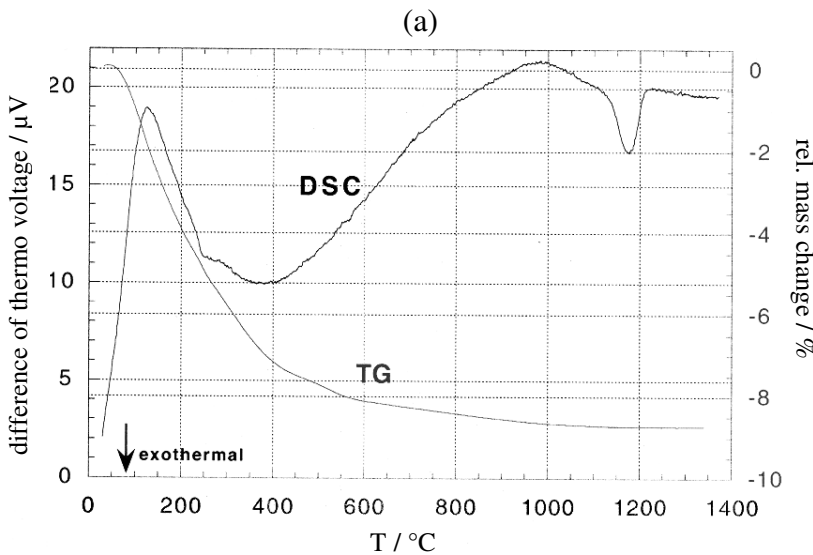(b) Nanosized alumina doped with ~ 6 mol% iron(III)-oxide crystallizes in the cubic γ-phase.

Fig. 6. Phase transformation of nanosized amorphous alumina measured with DSC/TG (a) and HT-XRD (b).
(a) In the DSC plot a phase transformation is seen at ~1200 °C, the typical temperature for the formation of α-alumina. The weight loss (TG-curve) is due to loss of surface water.

(b) In the HT-XRD spectra, the cubic γ-phase is the only one occurring up to 900 °C. The transformation to α-alumina starts at 1000 °C; at 1100 °C the cubic γ-phase is completely vanished.
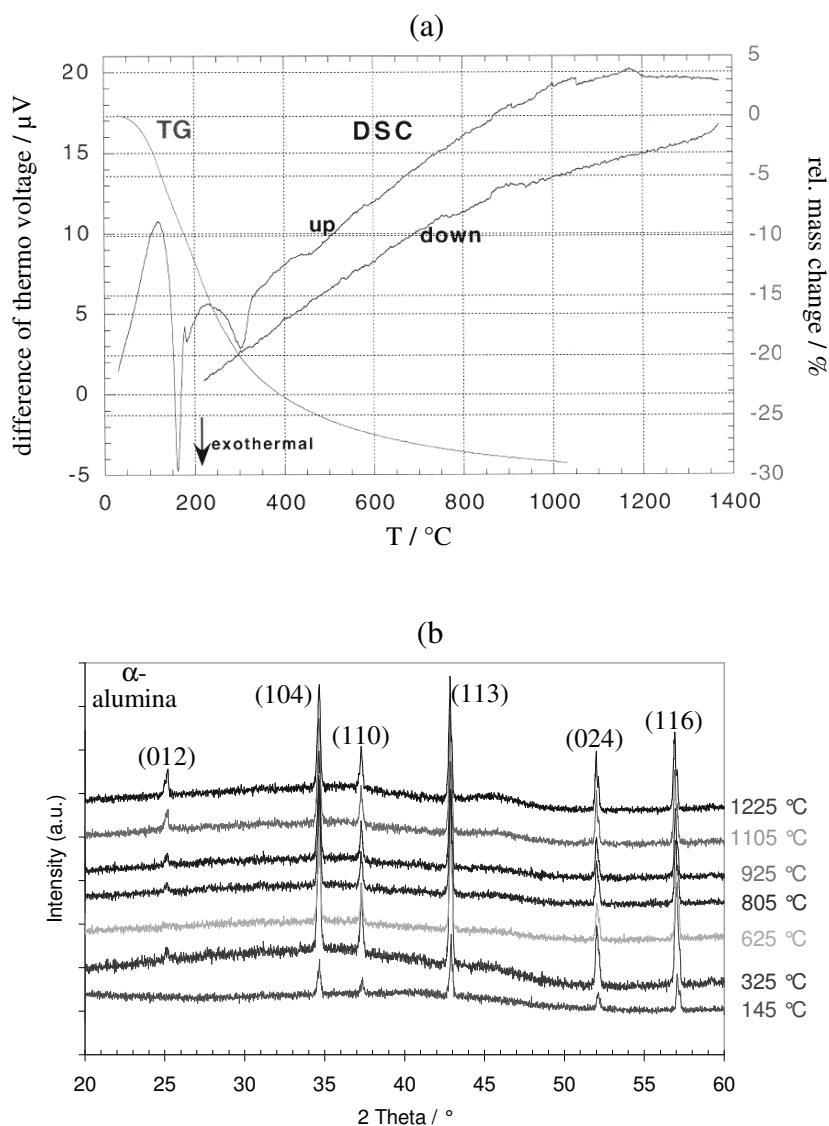
(a)

Fig. 7. Phase transformations for nanosized alumina doped with ~ 1 mol% iron(III)-oxide measured with DSC/TG (a) and HT-XRD (b).
(a) In the DSC plot the formation of the α-phase is found at 300 °C, which is surprisingly low. At higher temperatures, there are no indications for additional phase transformations. The weight loss (TG-curve) is attributed to the loss of surface water.

(b)

(b) In the HT-XRD spectra the low transformation temperature found in the DSC measurement is confirmed. Indications for the formation of α-alumina occur already at 145 °C. Metastable phases were not formed.

Summary

The Karlsruhe Microwave Plasma Process is capable to synthesize bare, coated, and in-situ doped nanoparticles with narrow particle size distribution in the range from 2 to 5 nm. The synthesized zirconia nanoparticles are crystalline with cubic structure. A further interesting feature is the high concentration of Schottky defects leading to a low relative density of only 0.61. Alumina nanoparticles are generally amorphous with very small amounts of the cubic γ-phase. The formation of the cubic γ-phase seems to be preferred using ~ 6 mol% iron(III))-oxide as a dopant. Small additions of iron(III)-oxide to alumina show severe influence to the temperature of phase transformation to α-alumina. This transformation temperature decreases from 1100 – 1200 °C for pure alumina down to 300 °C for alumina doped with ~ 1 mol% iron(III)-oxide. The transition from the amorphous state to the α-phase occurs without passing any metastable phase.

References

[1] D. Vollath, K.E. Sickafus: Nanostruct. Mater. Vol. 1 (1992), p. 427.

[2] D. Vollath, D.V. Szabó: Nanostruct. Mater. Vol. 3 (1994), p. 927.

[3] D. Vollath, D.V. Szabó: K.L. Choy [ed.] Innovative Processing of Films and Nanocrystalline Powders (Imperial College Press London) (2002), p. 219.

[4] D. Vollath, M. Forker, M. Hagelstein, D.V. Szabó: Mat. Res. Soc. Symp. Proc. (2001), p. 634, B7.7.1.

[5] S. Appel, R. Clasen, A. Chkourankov, H. Natter, R. Hempelmann, S. Schlabach, B. Xu, D. Vollath: 26th Ann. Conf. on Composites, Advanced Ceramics, Materials and Structures, Amer. Ceram. Soc. (2002), p. 585.

[6] A. Braun, R. Clasen, S. Schlabach, B. Xu, D. Vollath: 27th Ann. Meeting Int. Conf. on Advanced Ceramics & Composites (2003). To be published in Ceramic Transactions.

[7] S. Appel, R. Clasen, S. Schlabach, B. Xu, D. Vollath: 26th Ann. Conf. on Composites, Advanced Ceramics, Materials and Structures, Amer. Ceram. Soc. (2002), p. 609.